Electronic Journal of Biotechnology 41 (2019) 37–47

Contents lists available at ScienceDirect

Electronic Journal of Biotechnology

Research Article

Discovery and molecular analysis of conserved circRNAs from cashmere goat reveal their integrated regulatory network and potential roles in secondary hair follicle

Ronghuan Yin [a], Yanru Wang [a], Zeying Wang [a], Yubo Zhu [a], Yuyan Cong [a], Wei Wang [a], Liang Deng [a], Haiying Liu [a], Dan Guo [b], Wenlin Bai [a,*]

[a] College of Animal Science & Veterinary Medicine, Shenyang Agricultural University, Shenyang 110866, PR China
[b] Academy of Animal Husbandry Science of Liaoning Province, Liaoyang 130062, PR China

ARTICLE INFO

Article history:
Received 2 April 2019
Accepted 28 June 2019
Available online 9 July 2019

Keywords:
Anagen
Bioinformatics
Cashmere goat
CircRNA expression
Eukaryotic transcriptome
Expression pattern
MicroRNA
Regulatory network
Secondary hair follicle
Skin tissue
Telogen

ABSTRACT

Background: Circular RNAs, a novel class in the eukaryotic transcriptome, are characterized by the 3′ and 5′ ends that are covalently joined in a covalently closed loop without free ends. Circular RNAs are considerably stable molecules and act as microRNA sponges with regulatory potential to the protein-coding genes.
Results: Eight circular RNAs were found to be significantly upregulated at anagen skin tissue of cashmere goat compared with their counterparts at telogen. Rich and complex regulatory patterns were revealed among the eight upregulated circular RNAs at anagen and related miRNAs with their potential regulatory genes. The potential regulatory genes of eight upregulated circular RNAs at anagen were involved in several pathways related to the main physiological process of hair follicle, such as histone acetylation and axon. For chi_circ_1926, chi_circ_3541, chi_circ_0483, chi_circ_3196, and chi_circ_2092, overall, the relative expression in secondary hair follicle exhibited highly similar trends with their corresponding host genes during the different stages of the hair follicle cycle. However, the expression trends of chi_circ_0100, chi_circ_2829, and chi_circ_1967 were found to diverge from their corresponding host genes during the different stages of the hair follicle cycle.
Conclusions: A total of eighteen circular RNAs were identified and characterized from skin tissue of cashmere goat. The eight upregulated circular RNAs at anagen might have significant roles in the secondary hair follicle of cashmere goat. Our results would provide a novel regulatory layer to elucidate the molecular mechanisms underlying the development of secondary hair follicle and the growth of cashmere fiber in cashmere goat.
How to cite: Yin R, Wang Y, Wang Z, et al. Discovery and molecular analysis of conserved circRNAs from cashmere goat reveal their integrated regulatory network and potential roles in secondary hair follicle. Electron J Biotechnol 2019;41. https://doi.org/10.1016/j.ejbt.2019.06.004.

1. Introduction

Cashmere goats are characterized by a double fleece consisting of two distinct fiber types: the over hair and the under cashmere [1]. The hair is produced by primary hair follicle, whereas the cashmere is produced by secondary hair follicle, which is the main use of cashmere goats [2]. As is well known, the growth of cashmere fiber was regulated by the cyclic biological process of secondary hair follicle consisting of anagen, catagen, and telogen stages, which is under the control of photoperiod change along with the precise regulation of the endocrine system of cashmere goat [3,4]. Over the past few decades, regulatory factors involved in cashmere fiber growth have been investigated at several levels, including genes with methylation characterizations [5,6,7], microRNAs (miRNAs) [8,9,10], and lncRNAs [11,12,13,14]. Overall, however, the exact molecular regulatory mechanisms underlying cashmere growth have not yet been fully clarified. To this end, the discovery and characterization of novel regulation factors might be an alternative strategy to reveal molecular mechanisms of cashmere growth in cashmere goat. In recent years, a new class of the RNA molecules, called circular RNAs (circRNAs), has received particular attention in that they play a significant role in the regulation of gene expression [15,16,17]. CircRNAs are characterized by their unique structure, the 3′ and 5′ ends of which are covalently joined in a covalently closed loop without free ends differing from other types of RNA molecules [18,19]. Increasing lines of evidence indicate that circRNAs are expressed prevalently in the eukaryotic transcriptome [20,21,22], and thousands of circRNAs have been

* Corresponding author.
E-mail address: baiwenlin@syau.edu.cn (W. Bai).

https://doi.org/10.1016/j.ejbt.2019.06.004

Table 1
Details of the 18 putative circRNAs in this study and their corresponding host genes.

circRNA number[a]	Length of spliced sequence (nt)	Number of chromosome	Location on chromosome	Corresponding sequence ID in goat genome	Corresponding homology circRNA ID of human in circRNADb (length of spliced sequence, nt)	Identity with homology circRNA of human (%)	Host gene
chi_circ_0672	1360	Chromosome 2	113507839 to 113509198	NC_030809.1	hsa_circ_00233 (1360)	96	SP3
chi_circ_1967	1971	Chromosome 8	27805904 to 27807873	NC_030815.1	hsa_circ_22722 (1970)	91	BNC2
chi_circ_0433	1417	Chromosome 8	38569958 to 38571374	NC_030815.1	hsa_circ_13285 (1619)	94	KIAA2026
chi_circ_3277	1435	chromosome 9	28811280 to 28812714	NC_030816.1	hsa_circ_19222 (1435)	92	FOXO3
chi_circ_1947	1340	chromosome 9	59280910 to 59282249	NC_030816.1	hsa_circ_13228 (1341)	87	SLC2A12
chi_circ_2092	1049	chromosome 9	63980390 to 63981438	NC_030816.1	hsa_circ_12524 (1041)	89	HECA
chi_circ_1560	1130	chromosome 10	65986382 to 65987511	NC_030817.1	hsa_circ_01692 (1131)	92	MGA
chi_circ_3196	1834	chromosome 11	22619567 to 22621400	NC_030818.1	hsa_circ_10435 (1832)	90	SLC8A1
chi_circ_3541	1908	Chromosome 15	19007782 to 19008879	NC_030822.1	hsa_circ_24807 (1099)	95	HIPK3
chi_circ_0100	1619	Chromosome 18	23019634 to 23021252	NC_030825.1	hsa_circ_28162 (1616)	93	CHD9
chi_circ_1926	3887	Chromosome 21	41938604 to 41942490	NC_030828.1	hsa_circ_29011 (3885)	95	ARHGAP5
chi_circ_1690	3282	Chromosome 27	29023225 to 29026506	NC_030834.1	hsa_circ_25951 (3283)	84	FAT1
chi_circ_0373	1073	Chromosome 29	35660302 to 35661374	NC_030836.1	hsa_circ_02017 (1074)	94	ZBTB44
chi_circ_0175	1116	Chromosome 2	37921929 to 37923044	NC_030809.1	hsa_circ_10974 (1117)	92	KANSL1L
chi_circ_2829	1062	Chromosome 8	105101777 to 105102838	NC_030815.1	hsa_circ_01183 (1063)	87	PAPPA
chi_circ_0483	1515	Chromosome 11	13101422 to 13102936	NC_030818.1	hsa_circ_05103 (1519)	94	ZNF638
chi_circ_1176	1963	Chromosome 11	62684628 to 62686590	NC_030818.1	hsa_circ_28683 (1967)	90	AFTPH
chi_circ_1549	1147	Chromosome 27	22098436 to 22099582	NC_030834.1	hsa_circ_17568 (1148)	86	DLC1

[a] The genomic information of each putative circRNA was determined by mapping it to the reference genome of goat: ChIR_1.0, Reference Annotation Release 101 (http://www.goatgenome.org).

distinctly identified in various tissues across different species, such as human [23], pig [24], cattle [25,26] and chicken [27]. Investigations at a global scale of circRNAs indicated that a considerable degree of conservation exists among closely related species with a subset of circRNAs conserved even in the evolutionary distant species [28,29,30]. There is evidence that circRNAs can act as miRNA sponges, implying that circRNA may regulate finally the expression of protein-coding genes through a complex competing endogenous RNA (ceRNA) network: circRNA–miRNA–mRNA [22,31,32].

In humans, it was reported that circRNA mediates the role of skin mesenchymal stem cells in the pathogenesis of psoriasis [33]. In fur skin of mice, it was also demonstrated that several circRNAs were involved in the pigmentation and melanin-related pathways, such as circMagil and circSnx13 [34]. More recently, another investigation by Pang et al. [35] indicated that circular RNAs might play an important role in goat skin fibroblast cells in response to contagious ecthyma virus infection through the circRNA–miRNA–mRNA regulatory network. To date, however, little information is available about circRNAs in the skin tissue of cashmere goat, which might be essential for understanding the molecular mechanisms underlying cashmere fiber growth in cashmere goat.

In the present study, a total of eighteen conserved circRNAs were identified and characterized from skin tissue of cashmere goat. Of them, eight circRNAs were revealed to be significantly upregulated at anagen compared with those at telogen of the secondary hair follicle cycle. We further generated the regulatory network of these eight upregulated circRNAs at anagen with related signal pathway analysis through bioinformatics tools. In addition, we examined their expression pattern in the secondary hair follicle of cashmere goat during the hair follicle cycle along with the expression analysis of their corresponding host genes. The results from the present study would contribute to elucidating the regulatory characteristics and functional roles of the circRNAs in the development of secondary hair follicle and cashmere fiber growth in cashmere goat.

2. Materials and methods

2.1. Sources of sequences and samples

The experimental protocol was reviewed and approved by the Animal Experimental Committee of Shenyang Agricultural University. The analyzed eighteen sequences of putative circRNAs were obtained from a full-length transcriptome sequencing data on anagen skin tissue of cashmere goat (unpublished data), which was carried out using the single-molecule real-time sequencing technique [36]. A total of 876 circRNAs were predicted from the obtained sequencing data through taking the intersection of three identifying tools for circRNAs: CIRCexplorer2 [37], Find_circ [19], and CIRI [38]. A BLAST similarity searching for these obtained 876 sequences was performed in the comprehensive database for human circular RNAs: circRNADb (http://reprod.njmu.edu.cn/circrnadb). We found eighteen sequences were matched well to corresponding circRNAs of human with high identity of 84–96% (Table 1). Thus, the eighteen sequences were selected for further analysis in this study.

To preliminarily investigate their expression pattern of the eighteen putative circRNAs in the skin tissue of cashmere goat at anagen and telogen stages, we used the total RNA isolated from the skin tissue of Liaoning cashmere goat was according to the procedure described in detail in our previous study [2]. For further analysis of the expression characterization of the eight putative circRNAs (revealed to have higher expression at anagen than at telogen) along with the corresponding host genes in the secondary hair follicle of cashmere goat, three stages of the secondary hair follicle cycle were investigated, namely, anagen, catagen, and telogen. The total RNA was used, which was isolated from the secondary hair follicle of Liaoning cashmere goat according to the procedure given in our another investigation [11].

2.2. Sequences and regulatory network analysis of putative circRNAs with pathway enrichment of the potential regulatory genes through their target miRNAs

The potential open reading frames (ORFs) of the putative circRNAs were determined with the online service program: Coding Potential Assessment Tool (CPAT, http://lilab.research.bcm.edu/cpat/index.php). This CPAT program was also used for assessing the coding potential of putative circRNAs. The CPAT is an alignment-free approach; therefore, it was thought to be better in terms of sensitivity and specificity than alignment-based approaches, in that it performed the analysis through a logistic regression model based on pure sequence-based linguistic features, including ORF size, ORF coverage, Fickett test code statistic, and hexamer usage bias [39].

For generating the competitive endogenous RNA (ceRNA) regulatory network of the circRNAs, the target miRNAs were predicted

on each putative circRNA sequence using the miRDB program (http://www.mirdb.org). The miRDB, an online resource, was developed for miRNA target prediction along with functional annotations. In miRDB analysis, all the targets were predicted through analyzing thousands of interactions of miRNA-target from high-throughput sequencing data. Moreover, common features associated with miRNA binding and target downregulation have been identified and used to predict miRNA targets with machine learning methods [40]. Further, we predicted the target genes of the resultant miRNAs based on the use of the miRDB program. The ceRNA regulatory network of circRNAs was finally generated and visualized using Cytoscape software (version 2.8) [41].

Using the CluePedia Cytoscape plugin (http://www.ici.upmc.fr/cluepedia/), we performed the pathway enrichment analysis of the potential regulatory genes of putative circRNAs through their target miRNAs. The CluePedia Cytoscape plugin was developed for revealing new markers potentially associated with pathways, and it calculates linear and nonlinear statistical dependencies from experimental data [42]. Through the CluePedia Cytoscape plugin, genes can be connected and integrated into a network of pathways where new potential associations may be revealed through gene enrichments [42].

2.3. Designing of primers

A total of 29 pair primers were used in this study. To detect the expression of putative circRNAs, eighteen divergent primer pairs were designed using the CircPrimer program [43]. For analyzing the expression of the corresponding host genes of the circRNAs having higher expression at anagen than at telogen of skin tissue, eight convergent primer pairs were designed using Primer Premier 5.0 software (http://www.premierbiosoft.com). Additionally, in our previous investigation, three housekeeping genes, namely, *UBC*, *YWHAZ*, and *SDHA*, were confirmed to be suitable internal reference genes in the skin tissue of Liaoning cashmere goat [44]. Thus, they were used as combined internal references for normalizing the expression level of the putative circRNAs and the host genes in this study. Their corresponding primers were designed in our previous investigation [44], including *REF-UBC-1* versus *REF-UBC-2*, *REF-YWHAZ-1* versus *REF-YWHAZ-2*, and *REF-SDHA-1* versus *REF-SDHA-2*. All the used primers were commercially synthesized by Sangon Biotechnology Co., Ltd. (Shanghai, China) and were purified by polyacrylamide gel electrophoresis. The information of these primers is presented in Table S1.

2.4. Expression analysis of putative circRNAs and their corresponding host genes in skin tissue/secondary hair follicle of cashmere goat

To detect the expression of putative circRNAs in skin tissue/secondary hair follicle of cashmere goat, real-time PCRs were performed with SYBR® Green PCR Supermix (Bio-Rad, CA, USA) on a light Cycler 480 real-time PCR system (Roche Diagnostics, Mannheim, Germany). We reverse-transcribed the total cDNA with the PrimeScript™ 1st Strand cDNA Synthesis Kit (TaKaRa, Dalian, China) following the manufacturer's instructions. Real-time PCRs were performed in a 20 μL final volume containing SYBR® Green PCR Supermix 10 μL, each of divergent/convergent primers (10 mM) 0.8 μL, first-strand cDNA 2.0 μL, and PCR-grade double distilled ddH_2O water 6.4 μL. The cycling parameters were set as follows: an initial single cycle (95°C for 4 min), followed by 40 cycles (95°C for 20 s, 52–60°C for 20 s, and 72°C for 20 s). All amplifications were followed by melting curve analysis from 56 to 95°C with a ramp speed of 0.5°C per 10 s to confirm a single product being amplified in each primer set. Three replicates were run for all reactions. A negative control without a cDNA template was incorporated in each measurement. The relative expression levels were calculated by the $2^{-\Delta\Delta Ct}$ method [45].

2.5. Data analysis

In the relative expression analysis of putative circRNAs and their host genes, the geometric mean of *UBC*, *YWHAZ*, and *SDHA* was used as combined references, which was recommended in a previous study [44]. The normalized real-time PCR data were further processed according to the method described by Bionaz and Loor [46]. In brief, with the aim of estimating the standard error of the telogen period and preventing possible deviations, the normalized data were converted to obtain a perfect average of 1.0 at telogen where a proportional difference among biological replicates was left. We calculated the same proportional change at anagen/catagen for obtaining a fold change relative to telogen. The transformed expression data of circRNAs and their host genes were presented as $\log_2$ *n*-fold change relative to telogen. Data differences between/among groups were analyzed by one-way single-factor analysis of variance (ANOVA), and the mean values of data were compared with Duncan's multiple comparison method. The difference was considered statistically significant when the *P* value was less than 0.05. All data analyses were performed with SPSS 12.0 software (SPSS Inc., Chicago, IL, USA).

3. Results and discussion

3.1. Discovery and characterization of putative circRNAs and their expression pattern in skin tissue of cashmere goat

In previous investigations, it was demonstrated that circRNA sequences displayed a considerable degree of conservation among closely related species. Moreover, a small population of circRNAs were conserved even among the evolutionarily distant species [28,29,30]. Therefore, with the aim of identifying potential conservative circRNAs from the skin tissue of cashmere goat, the 876 predicted circRNAs from the sequencing data of the skin tissue of cashmere goat were subjected to BLAST search in the human circular RNA database: circRNADb. As shown in Table 1, there are 18 predicted circRNAs that are matched well to the different circRNAs of humans with high identity, that is, 86–96% (Table 1). The genomic information of the 18 putative circRNAs was determined by mapping them to the reference genome of goat (ChIR_1.0, Reference Annotation Release 101, http://www.goatgenome.org). In Table 1, we provided the all mapping information of the 18 putative circRNAs on goat reference genome. As observed from Table 1, several putative circRNAs are mapped onto the same chromosome, such as chi_circ_3277, chi_circ_1947 and chi_circ_2092 on the chromosome 9, as well as chi_circ_3196, chi_circ_0483, and chi_circ_1176 on chromosome 11, but they do not have any shared overlap region, which can be determined by the matching position information on the corresponding chromosomes. On the other hand, we also noted that all the 18 putative circRNAs were transcribed from their respective differential host genes of goat (Table 1).

Originally, circRNAs were thought to be noncoding RNAs; however, there is increasing evidence that some circRNAs can be translated into polypeptides with physiological function [47,48,49]. Thus, we evaluated bioinformatically the coding potential of the putative 18 circRNAs by the CPAT procedure along with a screening of their respective potential open reading frames (ORFs) in their sequences. As shown in Fig. 1a, each of them contained one ORF. Moreover, 12 putative circRNAs were revealed to have a final coding probability score more than the set cutoff value of 0.5, such as chi_circ_1967, chi_circ_0433, and chi_circ_2092 (Fig. 1b). These results could offer new insight into the investigation of coding potential of these putative circRNAs in skin tissue of cashmere goat. On the other hand, it was recently reported that the N^6-methyladenosine (m^6A) motif was required for circRNA to drive efficient initiation of protein translation [50]. In the present study, we showed that the twelve putative

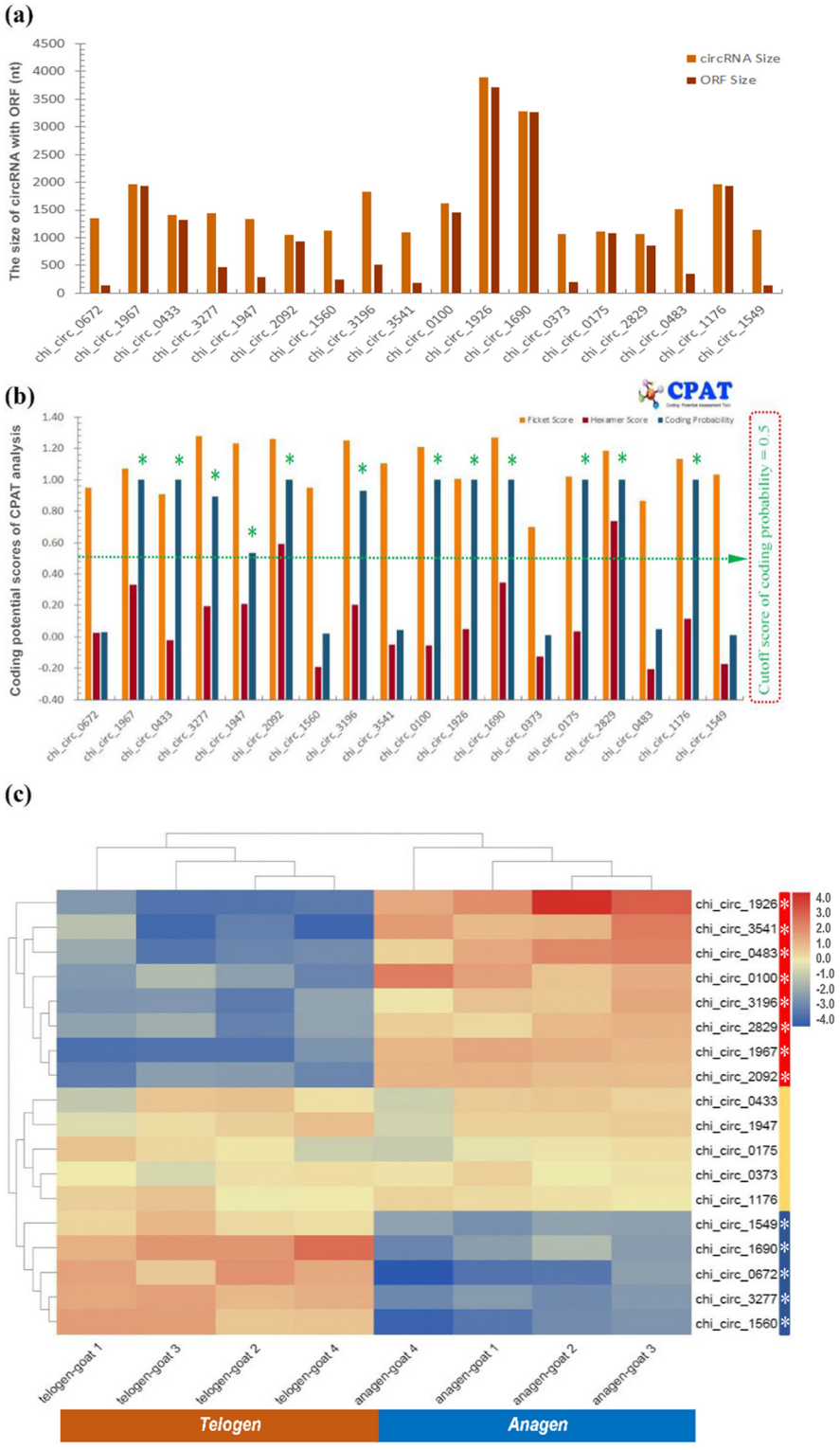

Fig. 1. Identification of putative circRNAs and their expression pattern in skin tissue of cashmere goat at anagen and telogen. (a) The potential ORF analysis of putative circRNAs as determined using the online service program: Coding Potential Assessment Tool (CPAT, http://lilab.research.bcm.edu/cpat/index.php). (b) Coding potential analysis of putative circRNAs as also performed using CPAT algorithm with the cutoff value for coding probability being set as 0.5, and the asterisk indicated the coding probability score of the corresponding circRNA is more than the cutoff value of 0.5. (c) Hierarchical clustering heat map of the analyzed circRNAs in skin tissue of cashmere goat at anagen and telogen that was generated based on the obtained real-time PCR data in this study, and the asterisk indicates significant difference of the corresponding circRNA in expression mean between anagen and telogen ($P < 0.05$).

circRNAs appear to have coding potential for polypeptides (Fig. 1a and b). Therefore, we strongly suggest that m^6A motifs on the twelve circRNAs should be investigated in the skin tissue of cashmere goats, which might mean further importance.

As is well known, real-time PCR technique is the gold standard in analyzing the expression level of various types of RNA species owing to its high sensitivity, specificity, and reproducibility [51]. With real-time technique, here, the expression level of the 18 putative circRNAs

was detected in the skin tissue of cashmere goat at both anagen and telogen of the secondary hair follicle cycle, and the obtained results are shown in Fig. 1c. Our data indicated that the 18 putative circRNAs were confirmed to be expressed in the skin tissue of cashmere at the two investigated stages: anagen and telogen. No significant deference was recorded in the relative expression of five circRNAs between telogen and anagen, including chi_circ_0433, chi_circ_1947, chi_circ_0175, chi_circ_0373, and chi_circ_1176 (Fig. 1c). Interestingly, considering the relatively stable expression of these five circRNAs during different stages of the secondary hair follicle cycle of cashmere goat, they have a potential value as internal references for circRNA expression analysis in the skin tissue of cashmere goat.

The remaining 13 circRNAs were revealed to exhibit significant differences in relative expression between anagen and telogen stages ($P < 0.05$, Fig. 1c). Among them, eight circRNAs were found to have significantly higher expression at anagen than at telogen including chi_circ_1926, chi_circ_3541, chi_circ_0483, chi_circ_0100, chi_circ_3196, chi_circ_2829, chi_circ_1967, and chi_circ_2092. In fact, the anagen is a crucial active phase for the formation and growth of cashmere fiber that is accompanied by the expression of hair-specific molecules such as keratins along with components of the inner root sheath [52,53]. Thus, it appears to become apparent that the eight upregulated circRNAs at the anagen stage may play significant roles in the formation and growth of cashmere fiber. This promotes us to undertake further investigation concerning the eight upregulated circRNAs at anagen including their regulatory network, pathway enrichment, and expression pattern in the secondary hair follicle of cashmere goat.

3.2. Regulatory network analysis of the upregulated circRNAs at anagen

In several investigations, recently, it was demonstrated that circRNAs can play their functional role through the ceRNA network: circRNA–miRNA–mRNA where circRNAs can sequester miRNAs, thereby reducing the number of active miRNAs, further protecting their target RNAs from repression [54,55]. Thus, the expression patterns of protein-coding genes were finally modulated by the interactions of circRNA–miRNA–mRNA. To understand the functional mechanisms of the circRNAs upregulated at anagen, here, we generated a ceRNA regulatory network for each circRNA using bioinformatics tools. The obtained results are presented in Fig. 2. As observed in Fig. 2, the ceRNA network showed the potential interaction relationships of each circRNA and its related miRNAs along with their target genes. Remarkably diverse regulatory relationships were revealed among the three types of RNA molecules: circRNA, miRNA, and mRNA. For example, the chi_circ_2092 may sequester five miRNAs, namely, miR-449b-5p, miR-449a, miR-4225, miR-504-3p, and miR-20b-3p, through which they further regulate individually or cooperatively the expression of several potential target genes such as *PPP1R11*, *SCN2B*, *BRWD3*, *FKBP1B*, and *MGAT4A* (Fig. 2b).

To better reveal the regulatory relationships among those eight circRNAs and the related miRNA along with their target genes, we merged the eight fractional networks (Fig. 2a–h) into an integrated ceRNA network using Cytoscape software. The incorporated ceRNA network is presented in Fig. 3, where the circRNAs, miRNAs, and target mRNAs are represented by red, yellow, and green filled circles, respectively. As shown in Fig. 3, a more diverse regulatory relationship was revealed among the circRNAs, miRNAs, and their target genes. For example, miR-149-5p was indicated to target two circRNAs: circRNA-1967 and circRNA-2092; it was also involved in the regulation of multiple genes including *CACHD1*, *IFFO2*, *DLL1*, *VPS53*, *ELP5*, *REP2S*, and *KIF2A* (Fig. 3). In fact, based on CLIP-seq data, the ceRNA interaction characterization of circRNA–miRNA–mRNA was also described and characterized according to those in several studies [56,57,58].

In the present study, the generated ceRNA network indicated the rich and complex regulatory patterns among the eight circRNAs and related miRNAs with their potential target genes. Interestingly, several miRNAs, which were predicted as targets on single or multiple circRNAs, were revealed to be significantly upregulated at anagen as compared to telogen/catagen of the secondary hair follicle cycle in cashmere goat, such as miR-331-3p ($P = 0.00000$), miR-378g ($P = 0.028752$), and miR-504-3p ($P = 0.00000$) [9,59]. This suggested that these miRNAs might be involved in the establishment of an optimal balance of gene expression at anagen, which might be required for the formation and growth of new cashmere shafts along with the expression of hair-specific molecules.

On the other hand, here, some genes predicted as the target gene of miRNAs, which were revealed to have potential binding sites on the analyzed circRNAs, were reported to play essential roles in the morphogenesis and development of hair follicle. For example, here, *IGFBP5* was predicted as the target gene of miR-608, miR-1275, and miR-5580-5p, of which, miR-1275 and miR-5580-5p were shown to have binding sites on chi_circ_1967 of cashmere goat, whereas *IGFBP5* was identified as a central regulator of hair shaft differentiation [60]. Similarly, the *IGF2BP1* and *KLF5* were predicted as target genes of miR-4500 and miR-153-3p, respectively. These two miRNAs, namely, miR-4500 and miR-153-3p, were shown to have binding sites on chi_circ_2829 and chi_circ_0100 of cashmere goat (Fig. 3). In previous investigations, it was suggested that *IGF2BP1* might be involved in the development of hair follicle [61], and the high expression of *KLF5* is observed in the basal layer of the inner root sheath and in matrix cell of hair follicles suggesting its functional roles in morphogenesis and growth of hair follicle [62]. In addition, *LIN28B*, predicted as a target gene of miR-4500 (revealed to have a binding site on chi_circ_2829), is a highly conserved paralog of *LIN28A* [63]. Although it is not yet known whether there play different physiological roles between *LIN28A* and *LIN28B*, it was demonstrated that *LIN28A* can promote hair growth by promoting anagen of the hair follicle cycle [63]. Taken together, it can be inferred that the upregulated circRNAs at anagen might play significant roles in regulating the expression of protein-coding genes in secondary hair follicle of cashmere goat through the interactional mechanisms of the ceRNA network.

3.3. Pathway enrichment on potential regulatory gene of upregulated circRNAs at anagen

From a functional point of view, integrating pathway network is essential for understanding the roles of regulatory factors in cellular processes and their dynamics [42]. Here, we performed a pathway enrichment analysis for the regulatory genes of upregulated circRNAs at anagen using the CluePedia Cytoscape plugin (http://www.ici.upmc.fr/cluepedia/). The enriched results are presented in Fig. 4. The analyzed genes and their corresponding pathways were simultaneously visualized in the CluePedia network where pathway terms and their associated genes share the same color. As shown in Fig. 4, the analyzed genes were significantly enriched in nine pathways, namely, regulation of transporter activity, trans-synaptic signaling, nuclear periphery, axon, positive regulation of organelle organization, negative regulation of cellular amide metabolic process, synapse organization, regulation of histone acetylation, and negative regulation of cardiocyte differentiation (Fig. 4). Of them, several pathways were involved in the main physiological process of hair follicle development. For example, it was demonstrated that histone acetylation can allow transcription factors to more easily access the DNA through an open chromatin structure and promotes exit from the hair follicle stem cell compartment [64,65,66]. Additionally, it was shown that axon signaling was necessary in driving the large-scale cellular rearrangements for the formation of hair follicle [67], and signal transduction regulation is an integral part in the hair follicle, including the ion transmembrane transporter activity [68]. Thus, it can be inferred that the analyzed genes might be involved in the

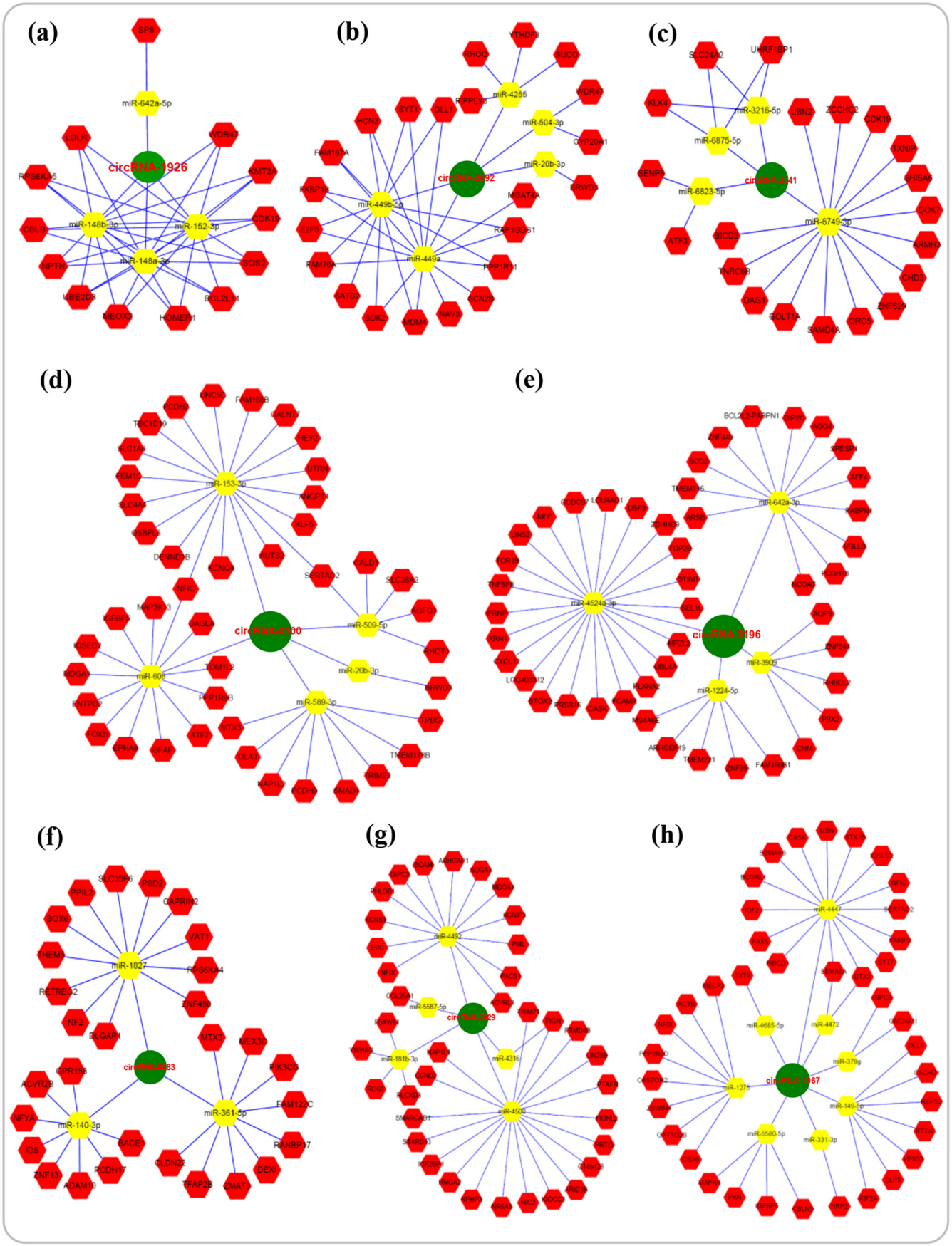

Fig. 2. The ceRNA regulatory network of each circRNA with higher expression in anagen skin tissue of the secondary hair follicle cycle. Green circles, yellow hexagons, and red hexagons were used for representing circRNAs, miRNAs, and potential target genes, respectively. (a) circRNA-1926 = chi_circ_1926, (b) circRNA-2092 = chi_circ_2092, (c) circRNA-3541 = chi_circ_3541, (d) circRNA-0100 = chi_circ_0100, (e) circRNA-3196 = chi_circ_3196, (f) circRNA-0483 = chi_circ_0483, (g) circ-2829 = chi_circ_2829, (h) circ-1967 = chi_circ_1967.

development and growth of hair follicle in cashmere goat where their role might be finally modified by the upregulated circRNAs at anagen.

3.4. Expression patterns of the upregulated circRNAs at anagen and their corresponding host genes in secondary hair follicle

Here, we further investigated the expression pattern of the eight upregulated circRNAs at anagen along with their corresponding host genes in the secondary hair follicle of cashmere goat during differential stages of the hair follicle cycle. The obtained results are presented in Fig. 5. Our data indicated that all the eight analyzed circRNAs along with their corresponding host genes were found to be expressed properly in the secondary hair follicle of cashmere goat at three stages of the hair follicle cycle: telogen, anagen, and catagen (Fig. 5). For chi_circ_1926, chi_circ_3541, chi_circ_0483, chi_circ_3196, and chi_circ_2092, overall, the relative quantitative expression exhibited highly similar trends with their corresponding host genes during the different stages of the hair follicle cycle (Fig. 5a, b, c, e and h). These results supported well the previous findings that the expression changes of most circRNAs are positively related to linear RNAs from the same host gene [29,69,70]. However, the expression trends of the chi_circ_0100, chi_circ_2829, and chi_circ_1967 were found to diverge from their corresponding host genes during the different stages of the hair follicle cycle (Fig. 5d, f, and g). In fact, this is not surprising in that previously some circRNAs were also found to even oppose the linear counterparts of the corresponding host gene in a dynamic manner [29,69]. Highly similar with those observed in skin tissue (Fig. 1c), the expression of the eight analyzed circRNAs was significantly upregulated at anagen of the secondary hair follicle in comparison to that at telogen (Fig. 5).

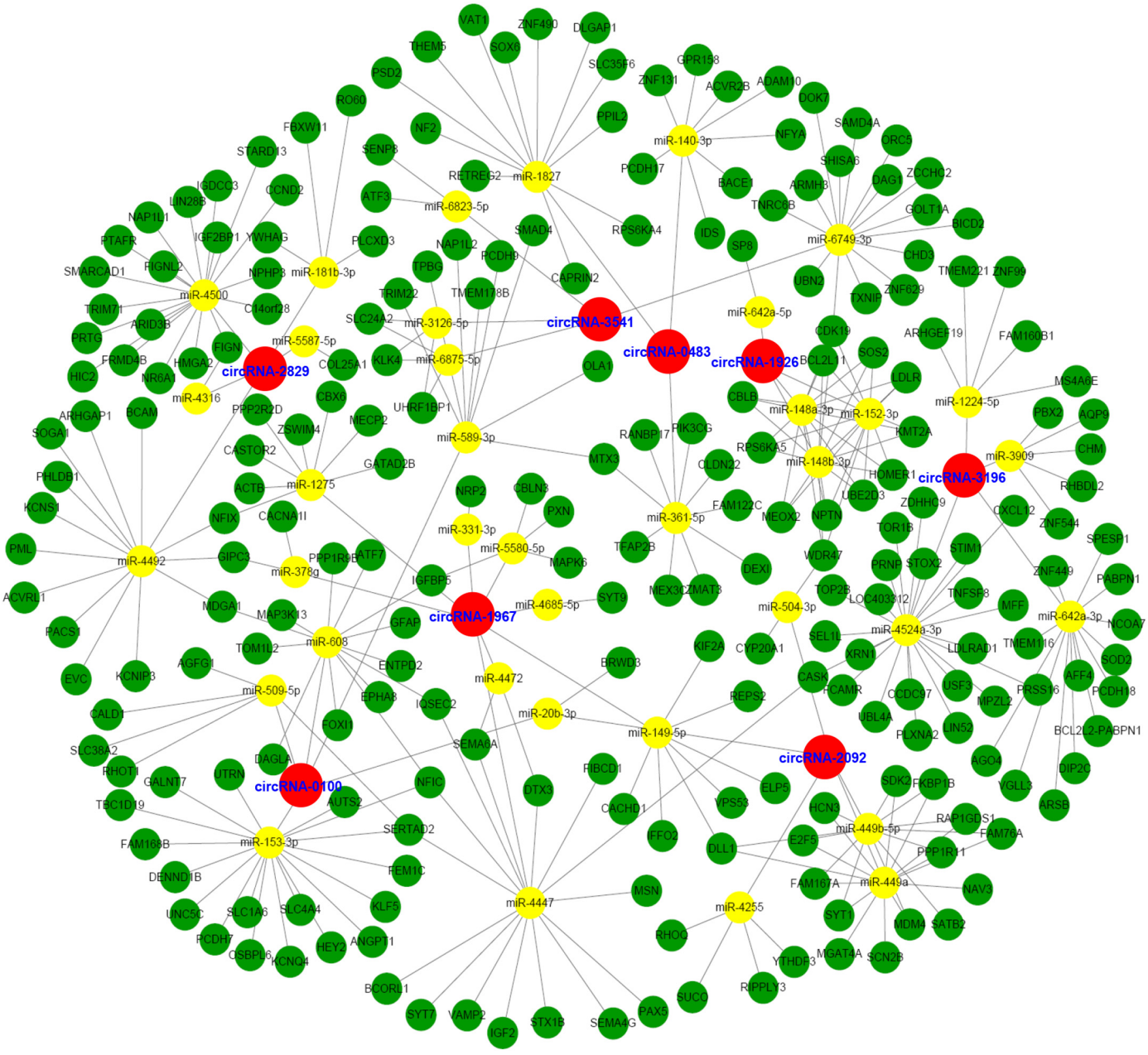

Fig. 3. Integrated regulatory network of eight circRNAs (circRNA-1926, circRNA-2092, circRNA-3541, circRNA-0100, circRNA-3196, circRNA-0483, circ-2829, and circ-1967) with higher expression in anagen skin tissue of the secondary hair follicle cycle. Red circles, yellow circles, and green circles represent circRNAs, miRNAs, and potential target genes, respectively. circRNA-1926 = chi_circ_1926, circRNA-2092 = chi_circ_2092, circRNA-3541 = chi_circ_3541, circRNA-0100 = chi_circ_0100, circRNA-3196 = chi_circ_3196, circRNA-0483 = chi_circ_0483, circ-2829 = chi_circ_2829, circ-1967 = chi_circ_1967.

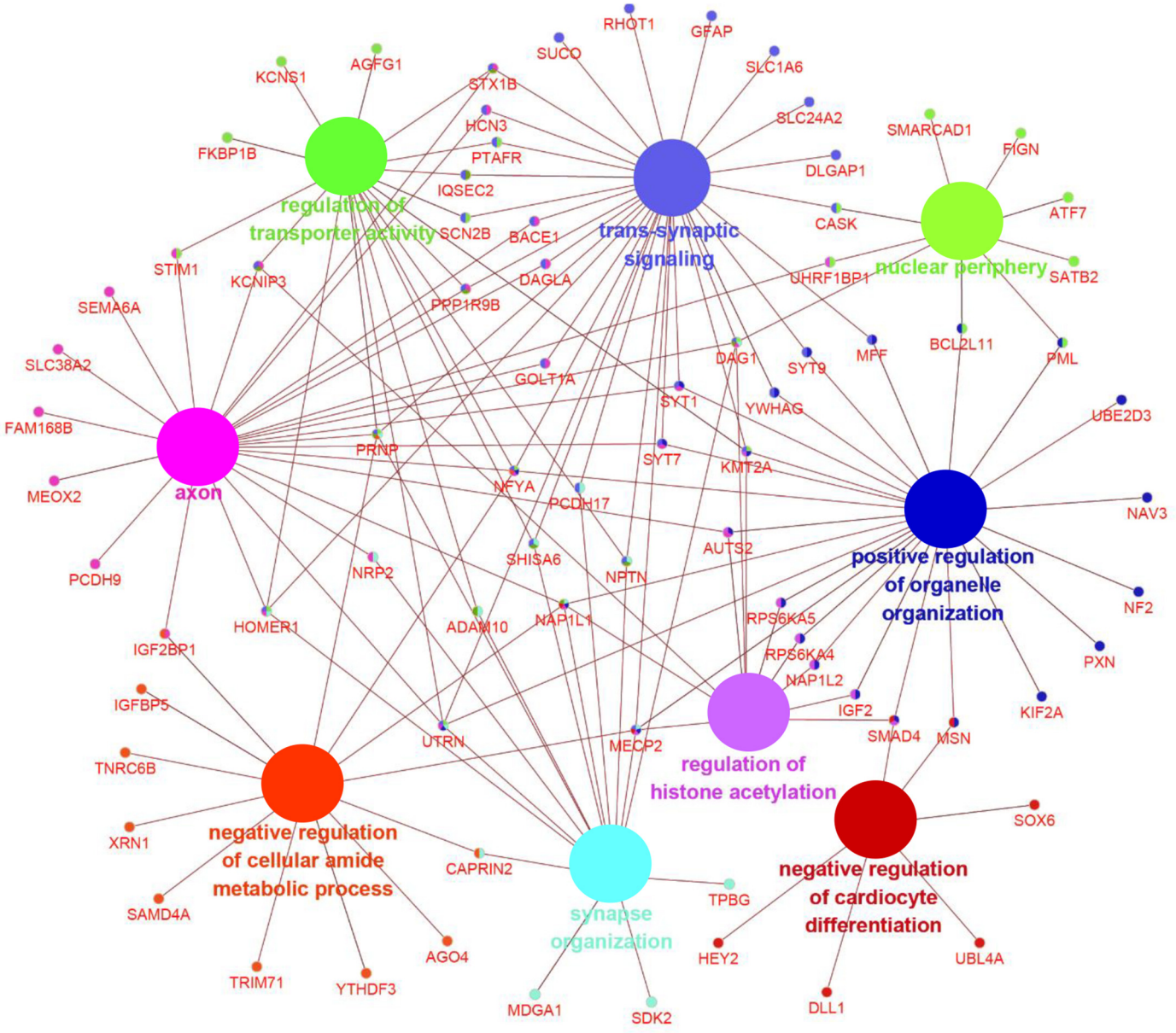

Fig. 4. Pathway enrichment analysis for the regulatory genes of upregulated circRNAs in anagen skin tissue of the secondary hair follicle cycle. The enrichment was performed by the CluePedia Cytoscape plugin (http://www.ici.upmc.fr/cluepedia/). The significantly enriched genes and their corresponding pathways were simultaneously visualized in the CluePedia network where pathway terms and their associated genes share the color.

Moreover, our analysis also confirmed that the expression of their corresponding host genes was the case in the secondary hair follicle of cashmere goat (Fig. 5).

In mice, it was demonstrated that *BNC2*, the host gene of chi_circ_1926, was largely expressed in the basal layer of the outer root sheath and the matrix of hair follicle at anagen and confirmed that it plays an important role in the regeneration and development of the hair follicle [71]. The *PAPPA* (the host gene of chi_circ_2829), an *IGFBP4* metalloproteinase, is expressed in human hair follicle and it can amplify the bioavailability of local *IGF1* through cleaving the inhibitory *IGFBP4* [72], whereas *IGF1* was demonstrated to possess important functions in the development and growth of hair follicles [73,74,75]. Further, as a member of the *ZNF* family, although the functional significance of *ZNF638* (the host gene of chi_circ_0483) needs to be further clarified in the physiological process of hair follicle, several members of this family were identified to act as key regulators in the secondary hair follicle of cashmere goat, including *ZNF704*, *ZNF667*, *ZNF454*, *ZNF407*, *ZNF347*, and *ZNF264* [76]. This suggested that the significantly upregulated expression of *ZNF638* at anagen of the secondary hair follicle of cashmere goat might mean further importance. Thus, it can be inferred that the three circRNAs (chi_circ_1926, chi_circ_2829, and chi_circ_0483) along with their corresponding host genes (*BNC2*, *PAPPA*, and *ZNF638*) might have certain functional roles in the development of secondary hair follicle and cashmere fiber growth through constituting perfect regulatory pairs.

On the other hand, the cell proliferation and growth are important physiological activities at the anagen stage of the secondary hair follicle in cashmere goat [74,75], during which several signaling pathways are involved in the proliferation and growth for the development of hair follicle, such as Wnt [77], IGF [74,75], NF-κB [78], Notch, and JAK–STAT [79], and their interplay is essential between epithelial and mesenchymal cells [78]. In this study, our data indicated that *ARHGAP5*, *HIPK3*, *CHD9*, *SLC8A1*, and *HECA*, (being the corresponding host genes of circRNAs-1926, -3541, -0100, -3196, and, -2092, respectively) were significantly upregulated at anagen of the

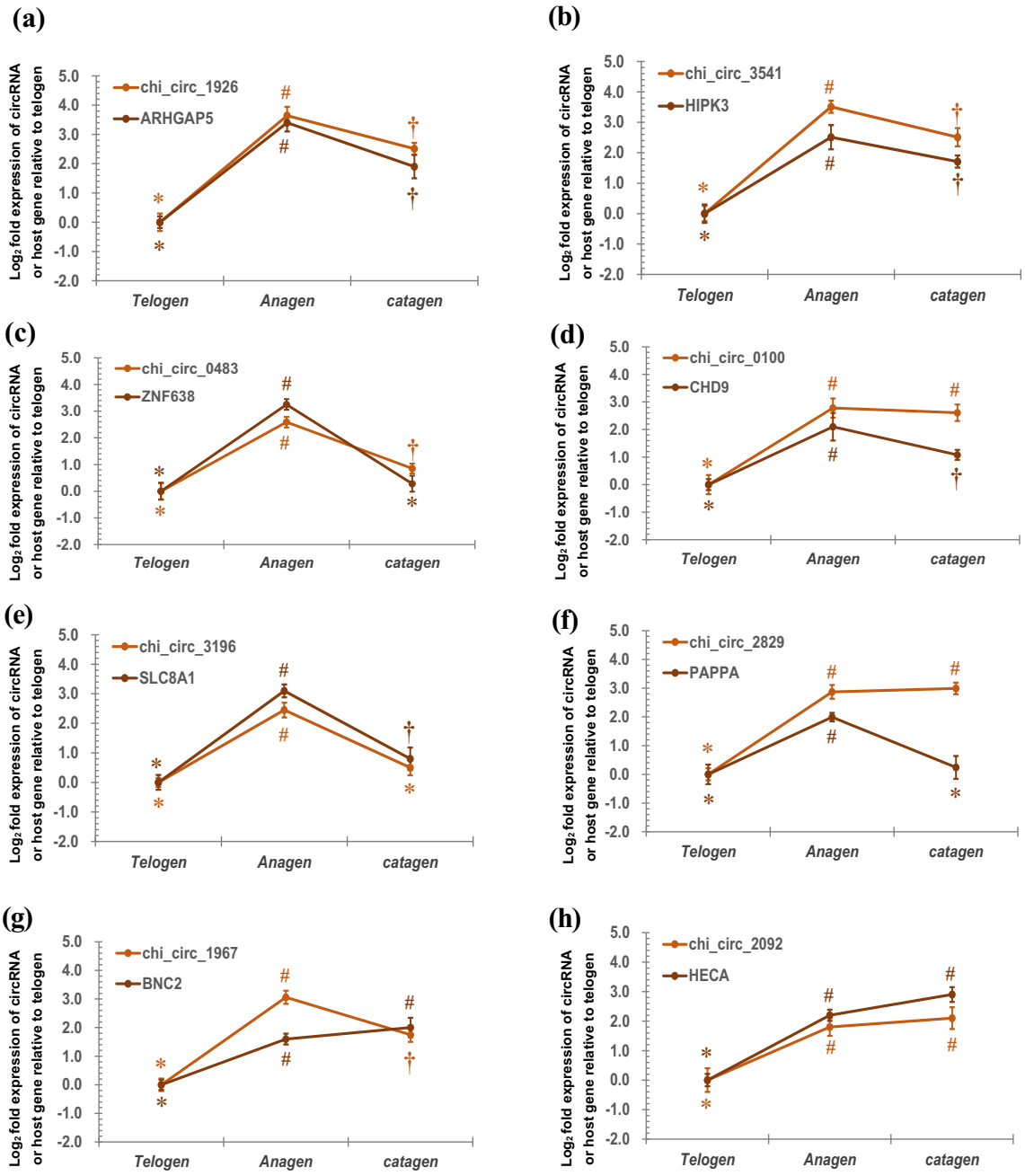

Fig. 5. Expression pattern of the eight upregulated circRNAs along with their corresponding host genes in the secondary hair follicle of cashmere goat during the hair follicle cycle. Blue and yellow indicate each circRNA and its host gene to denote their expression change. Error bar indicates SEM within the group. Different symbols (*, #, and †) among telogen, anagen, and catagen stages indicate significant difference ($P < 0.05$).

secondary hair follicle as compared to counterparts of telogen (Fig. 5a, b, d, e and h). In previous investigations, it was shown that the *ARHGAP5* can interact with IGF signings and be essentially involved in regulating both cell growth and differentiation [80,81]. The circ-HIPK3 that is derived from the *HIPK3* gene was found to significantly promote cell growth [23], and the *CHD9* can regulate activation of Notch/NF-B signal pathways through binding to miR-208a [82], whereas, the *SLC8A1* (also known as *NCX1*) is a regulator of Ca^{2+} concentration and is related to Wnt signaling by affecting Ca^{2+} concentration [83]. The *HECA* is involved in the Wnt/beta-catenin pathway [84,85] where a specific transcriptional program is induced by beta-catenin-dependent Wnt signaling that further controls the main aspects of cellular behavior, such as growth and differentiation [86]. Consequently, taken together with our results, an intriguing possibility was raised that *ARHGAP5*, *HIPK3*, *CHD9*, *SLC8A1*, and *HECA* along with their corresponding circRNAs (chi_circ_1926, chi_circ_3541, chi_circ_0100, chi_circ_3196, and chi_circ_2092) might constitute a novel regulatory layer in the cell proliferation and growth of secondary hair follicle of cashmere goat during the anagen stage.

In addition, our data indicated that three circRNAs, namely, chi_circ_0100, chi_circ_2829, and chi_circ_2092, were expressed at a higher level in the catagen stage, which is highly similar to those of the anagen stage (Fig. 5d, f and h). In fact, the catagen is a short transition phase lasting for only one month (January) in cashmere goat [87]. Therefore, we speculate that these three circRNAs (chi_circ_0100, chi_circ_2829, and chi_circ_2092) might also act as regulators in the transition of secondary hair follicle from catagen to telogen.

In conclusion, herein, we identified and characterized eighteen conserved circRNAs from the skin tissue of cashmere goat, of which eight circRNAs were found to be significantly upregulated at anagen skin tissue of cashmere goat when compared with their counterparts at telogen. We further generated the integrated regulatory network of the eight upregulated circRNAs with signal pathway enrichment analysis. We also investigated their expression pattern in the secondary hair follicle of cashmere goat during the hair follicle cycle along with the expression analysis of the corresponding host genes. The results from the present study would provide a novel regulatory layer to elucidate the molecular mechanisms underlying the development of secondary hair follicle and the growth of cashmere fiber in cashmere goat.

Financial support

The work was supported financially by grants from the National Natural Science Foundation of China (No. 31872325, No. 31672388, and No. 31802038); Key Project Foundation of Educational Department of Liaoning Province, China (No. LSNZD201606); Innovative Talent Support Program Foundation of Universities and Colleges in Liaoning Province, China (LR2016035); and Science and Technology Innovation Talent Support Foundation for Young and Middle-aged People of Shenyang City, China (RC170447).

Conflict of interest

The authors declare that there are no conflicts of interest.

Supplementary material

https://doi.org/10.1016/j.ejbt.2019.06.004

References

[1] Ji XY, Wang JX, Liu B, et al. Comparative transcriptome analysis reveals that a ubiquitin-mediated proteolysis pathway is important for primary and secondary hair follicle development in cashmere goats. PLoS One 2016;11(10):e0156124. https://doi.org/10.1371/journal.pone.0156124 PMid: 27695037.
[2] Bai WL, Dang YL, Wang JJ, et al. Molecular characterization, expression and methylation status analysis of BMP4 gene in skin tissue of Liaoning cashmere goat during hair follicle cycle. Genetica 2016;144(4):457–67. https://doi.org/10.1007/s10709-016-9914-1 PMid: 27406581.
[3] Kloren WRL, Norton BW, Waters MJ. Fleece growth in Australian cashmere goats. III. The seasonal patterns of cashmere and hair growth, and association with growth hormone, prolactin and thyroxine in blood. Aust J Agr Res 1993;44(5):1035–50. https://doi.org/10.1071/ar9931035.
[4] Wu J, Zhang Y, Zhang J, et al. Hoxc13/β-catenin correlation with hair follicle activity in cashmere goat. J Integr Agric 2012;11(7):1159–66. https://doi.org/10.1016/s2095-3119(12)60110-5.
[5] Bai WL, Yin RH, Yin RL, et al. IGF1 mRNA splicing variants in Liaoning cashmere goat: identification, characterization, and transcriptional patterns in skin and visceral organs. Anim Biotechnol 2013;24(2):81–93. https://doi.org/10.1080/10495398.2012.750245. PMid:23534956.
[6] Fan YX, Wu RB, Qiao X, et al. Hair follicle transcriptome profiles during the transition from anagen to catagen in Cashmere goat (*Capra hircus*). Genet Mol Res 2015;14(4):17904–15. https://doi.org/10.4238/2015.December.22.15 PMid: 26782436.
[7] Bai WL, Wang JJ, Yin RH, et al. Molecular characterization of HOXC8 gene and methylation status analysis of its exon 1 associated with the length of cashmere fiber in Liaoning cashmere goat. Genetica 2017;145(1):115–26. https://doi.org/10.1007/s10709-017-9950-5 PMid: 28093668.
[8] Liu Z, Xiao H, Li H, et al. Identification of conserved and novel microRNAs in cashmere goat skin by deep sequencing. PLoS One 2012;7(12):e50001. https://doi.org/10.1371/journal.pone.0050001 PMid: 23236360.
[9] Yuan C, Wang X, Geng R, et al. Discovery of cashmere goat (*Capra hircus*) microRNAs in skin and hair follicles by Solexa sequencing. BMC Genomics 2013;14:511. https://doi.org/10.1186/1471-2164-14-511 PMid: 23889850.
[10] Wang S, Ge W, Luo Z, et al. Integrated analysis of coding genes and non-coding RNAs during hair follicle cycle of cashmere goat (*Capra hircus*). BMC Genomics 2017;18(1):767. https://doi.org/10.1186/s12864-017-4145-0 PMid: 29020916.
[11] Zhu YB, Wang ZY, Yin RH, et al. A lncRNA-H19 transcript from secondary hair follicle of Liaoning cashmere goat: identification, regulatory network and expression regulated potentially by its promoter methylation. Gene 2018;641:78–85. https://doi.org/10.1016/j.gene.2017.10.028 PMid: 29054756.
[12] Bai WL, Zhao SJ, Wang ZY, et al. LncRNAs in secondary hair follicle of cashmere goat: identification, expression, and their regulatory network in Wnt signaling pathway. Anim Biotechnol 2018;29(3):199–211. https://doi.org/10.1080/10495398.2017.1356731 PMid: 28846493.
[13] Jin M, Cao M, Cao Q, et al. Long noncoding RNA and gene expression analysis of melatonin-exposed Liaoning cashmere goat fibroblasts indicating cashmere growth. Naturwissenschaften 2018;105(9–10):60. https://doi.org/10.1007/s00114-018-1585-6 PMid: 30291450.
[14] Jiao Q, Yin RH, Zhao SJ, et al. Identification and molecular analysis of a lncRNA-HOTAIR transcript from secondary hair follicle of cashmere goat reveal integrated regulatory network with the expression regulated potentially by its promoter methylation. Gene 2019;688:182–92. https://doi.org/10.1016/j.gene.2018.11.084 PMid: 30521888.
[15] Ebbesen KK, Hansen TB, Kjems J. Insights into circular RNA biology. RNA Biol 2016;14(8):1035–45. https://doi.org/10.1080/15476286.2016.1271524 PMid: 27982727.
[16] Wang H, Xiao Y, Wu L, et al. Comprehensive circular RNA profiling reveals the regulatory role of the circRNA-000911/miR-449a pathway in breast carcinogenesis. Int J Oncol 2018;52(3):743–54. https://doi.org/10.3892/ijo.2018.4265 PMid: 29431182.
[17] Gong GH, An FM, Wang Y, et al. Comprehensive circular RNA profiling reveals the regulatory role of the CircRNA-0067835/miR-155 pathway in temporal lobe epilepsy. Cell Physiol Biochem 2018;51(3):1399–409. https://doi.org/10.1159/000495589 PMid: 30485839.
[18] Hansen TB, Wiklund ED, Bramsen JB, et al. MiRNA-dependent gene silencing involving Ago2-mediated cleavage of a circular antisense RNA. EMBO J 2011;30(21):4414–22. https://doi.org/10.1038/emboj.2011.359 PMid: 21964070.
[19] Memczak S, Jens M, Elefsinioti A, et al. Circular RNAs are a large class of animal RNAs with regulatory potency. Nature 2013;495(7441):333–8. https://doi.org/10.1038/nature11928 PMid: 23446348.
[20] Glazar P, Papavasileiou P, Rajewsky N. CircBase: a database for circular RNAs. RNA 2014;20(11):1666–70. https://doi.org/10.1261/rna.043687.113 PMid: 25234927.
[21] Wang X, Li C, Gao X, et al. Preparation of small RNAs using rolling circle transcription and site-specific RNA disconnection. Mol Ther Nucleic Acids 2015;4:e215. https://doi.org/10.1038/mtna.2014.66 PMid: 25584899.
[22] Ma HB, Yao YN, Yu JJ, et al. Extensive profiling of circular RNAs and the potential regulatory role of circRNA-000284 in cell proliferation and invasion of cervical cancer via sponging miR-506. Am J Transl Res 2018;10(2):592–604. [PMid: 29511454].
[23] Zheng Q, Bao C, Guo W, et al. Circular RNA profiling reveals an abundant circHIPK3 that regulates cell growth by sponging multiple miRNAs. Nat Commun 2016;7(11215). https://doi.org/10.1038/ncomms11215 PMid: 27050392.
[24] Liang G, Yang Y, Niu G, et al. Genome-wide profiling of *Sus scrofa* circular RNAs across nine organs and three developmental stages. DNA Res 2017;24(5):523–35. https://doi.org/10.1093/dnares/dsx022 PMid: 28575165.
[25] Zhang C, Wu H, Wang Y, et al. Circular RNA of cattle casein genes are highly expressed in bovine mammary gland. J Dairy Sci 2016;99(6):4750–60. https://doi.org/10.3168/jds.2015-10381 PMid: 27040791.
[26] Gao Y, Wu M, Fan Y, et al. Identification and characterization of circular RNAs in Qinchuan cattle testis. R Soc Open Sci 2018;5(7):180413. https://doi.org/10.1098/rsos.180413 PMid: 30109096.
[27] Ouyang H, Chen X, Wang Z, et al. Circular RNAs are abundant and dynamically expressed during embryonic muscle development in chickens. DNA Res 2018;25(1):71–86. https://doi.org/10.1093/dnares/dsx039 PMid: 29036326.
[28] Guo JU, Agarwal V, Guo H, et al. Expanded identification and characterization of mammalian circular RNAs. Genome Biol 2014;15(7):409. https://doi.org/10.1186/s13059-014-0409-z PMid: 25070500.
[29] Rybak-Wolf A, Stottmeister C, Glažar P, et al. Circular RNAs in the mammalian brain are highly abundant, conserved, and dynamically expressed. Mol Cell 2015;58(5):870–85. https://doi.org/10.1016/j.molcel.2015.03.027 PMid: 25921068.
[30] Dang Y, Yan L, Hu B, et al. Tracing the expression of circular RNAs in human pre-implantation embryos. Genome Biol 2016;17(1):130. https://doi.org/10.1186/s13059-016-0991-3 PMid: 27315811.
[31] Hammond SM. Soaking up small RNAs. Nat Methods 2007;4(9):694–5. https://doi.org/10.1038/nmeth0907-694 PMid: 17762876.
[32] Jin X, Feng CY, Xiang Z, et al. CircRNA expression pattern and circRNA-miRNA-mRNA network in the pathogenesis of nonalcoholic steatohepatitis. Oncotarget 2016;7(41):66455–67. https://doi.org/10.18632/oncotarget.12186 PMid: 27677588.
[33] Liu R, Chang W, Li J, et al. Mesenchymal stem cells in psoriatic lesions affect the skin microenvironment through circular RNA. Exp Dermatol 2019;28(3):292–9. https://doi.org/10.1111/exd.13890 PMid: 30664808.
[34] Zhu Z, Li Y, Liu W, et al. Comprehensive circRNA expression profile and construction of circRNA-associated ceRNA network in fur skin. Exp Dermatol 2018;27(3):251–7. https://doi.org/10.1111/exd.13502 PMid: 29377327.
[35] Pang F, Zhang M, Yang X, et al. Genome-wide analysis of circular RNAs in goat skin fibroblast cells in response to Orf virus infection. PeerJ 2019;7:e6267. https://doi.org/10.7717/peerj.6267 PMid: 30697481.
[36] Eid J, Fehr A, Gray J, et al. Real-time DNA sequencing from single polymerase molecules. Science 2009;323(5910):133–8. https://doi.org/10.1126/science.1162986 PMid: 19023044.
[37] Dong R, Ma XK, Chen LL, et al. Genome-wide annotation of circRNAs and their alternative back-splicing/splicing with CIRCexplorer pipeline. Methods Mol Biol 1870;2019:137–49. https://doi.org/10.1007/978-1-4939-8808-2_10 PMid: 30539552.
[38] Gao Y, Wang J, Zhao F. CIRI: an efficient and unbiased algorithm for *de novo* circular RNA identification. Genome Biol 2015;16(1):4. https://doi.org/10.1186/s13059-014-0571-3 PMid: 25583365.
[39] Wang L, Park HJ, Dasari S, et al. CPAT: coding-potential assessment tool using an alignment-free logistic regression model. Nucleic Acids Res 2013;41(6):e74. https://doi.org/10.1093/nar/gkt006 PMid: 23335781.

[40] Wong N, Wang X. MiRDB: an online resource for microRNA target prediction and functional annotations. Nucleic Acids Res 2015;43(Database issue):D146–52. https://doi.org/10.1093/nar/gku1104 PMid: 25378301.
[41] Smoot M, Ono K, Ruscheinski J, et al. Cytoscape 2.8: new features for data integration and network visualization. Bioinformatics 2011;27(3):431–2. https://doi.org/10.1093/bioinformatics/btq675 PMid: 21149340.
[42] Bindea G, Galon J, Mlecnik B, et al. CluePedia Cytoscape plugin: pathway insights using integrated experimental and *in silico* data. Bioinformatics 2013;29(5):661–3. https://doi.org/10.1093/bioinformatics/btt019 PMid: 23325622.
[43] Zhong S, Wang J, Zhang Q, et al. CircPrimer: a software for annotating circRNAs and determining the specificity of circRNA primers. BMC Bioinformatics 2018;19(1):292. https://doi.org/10.1186/s12859-018-2304-1 PMid: 30075703.
[44] Bai WL, Yin RH, Yin RL, et al. Selection and validation of suitable reference genes in skin tissue of Liaoning cashmere goat during hair follicle cycle. Livest Sci 2014;161:28–35. https://doi.org/10.1016/j.livsci.2013.12.031.
[45] Livak KJ, Schmittgen TD. Analysis of relative gene expression data using real-time quantitative PCR and the $2^{-\Delta\Delta Ct}$ method. Methods 2001;25(4):402–8. https://doi.org/10.1006/meth.2001.1262 PMid: 11846609.
[46] Bionaz M, Loor JJ. ACSL1, AGPAT6, FABP3, LPIN1 and SLC27A6 are the most abundant isoforms in bovine mammary tissue and their expression is affected by stage of lactation. J Nutr 2008;138(6):1019–24. https://doi.org/10.1093/jn/138.6.1019 PMid: 18492828.
[47] Legnini I, Di Timoteo G, Rossi F, et al. Circ-ZNF609 is a circular RNA that can be translated and functions in myogenesis. Mol Cell 2017;66(1):22–37. https://doi.org/10.1016/j.molcel.2017.02.017 PMid: 28344082.
[48] Pamudurti NR, Bartok O, Jens M, et al. Translation of circRNAs. Mol Cell 2017;66(1):9–21.e7. https://doi.org/10.1016/j.molcel.2017.02.021 PMid: 28344080.
[49] Chen R, Jiang T, Lei S, et al. Expression of circular RNAs during C2C12 myoblast differentiation and prediction of coding potential based on the number of open reading frames and N^6-methyladenosine motifs. Cell Cycle 2018;17(14):1832–45. https://doi.org/10.1080/15384101.2018.1502575 PMid: 30080426.
[50] Yang Y, Fan X, Mao M, et al. Extensive translation of circular RNAs driven by N (6)-methyladenosine. Cell Res 2017;27(5):626–41. https://doi.org/10.1038/cr.2017.31 PMid: 28281539.
[51] Yadav P, Singh DD, Mukesh M, et al. Identification of suitable housekeeping genes for expression analysis in mammary epithelial cells of buffalo (*Bubalus bubalis*) during lactation cycle. Livest Sci 2012;147(1–3):72–6. https://doi.org/10.1016/j.livsci.2012.04.004.
[52] Paus K, Muller-Rover S. A comprehensive guide for the recognition classification of distinct stages of hair follicle morphogenesis. J Invest Dermatol 1999;113(4):523–32. https://doi.org/10.1046/j.1523-1747.1999.00740.x PMid: 10504436.
[53] Sharov AA, Sharova TY, Mardaryev AN, et al. Bone morphogenetic protein signaling regulates the size of hair follicles and modulates the expression of cell cycle-associated genes. Proc Natl Acad Sci U S A 2006;103(48):18166–71. https://doi.org/10.1073/pnas.0608899103 PMid: 17114283.
[54] Wei X, Li H, Yang J, et al. Circular RNA profiling reveals an abundant circLMO7 that regulates myoblasts differentiation and survival by sponging miR-378a-3p. Cell Death Dis 2017;8(10):e3153. https://doi.org/10.1038/cddis.2017.541 PMid: 29072698.
[55] Li H, Yang J, Wei X, et al. CircFUT10 reduces proliferation and facilitates differentiation of myoblasts by sponging miR-133a. J Cell Physiol 2018;233(6):4643–51. https://doi.org/10.1002/jcp.26230 PMid: 29044517.
[56] Li JH, Liu S, Zhou H, et al. StarBase v2.0: decoding miRNA-ceRNA, miRNA-ncRNA and protein-RNA interaction networks from large-scale CLIP-Seq data. Nucleic Acids Res 2014;42(Database issue):D92–7. https://doi.org/10.1093/nar/gkt1248 PMid: 24297251.
[57] Dudekula DB, Panda AC, Grammatikakis I, et al. CircInteractome: a web tool for exploring circular RNAs and their interacting proteins and microRNAs. RNA Biol 2016;13(1):34–42. https://doi.org/10.1080/15476286.2015.1128065 PMid: 26669964.
[58] Zhang XQ, Yang JH. Discovering circRNA-microRNA interactions from CLIP-Seq data. Methods Mol Biol 2018;1724:193–207. https://doi.org/10.1007/978-1-4939-7562-4_16 PMid: 29322451.
[59] Zhou GX, Kang DJ, Ma S, et al. Integrative analysis reveals ncRNA-mediated molecular regulatory network driving secondary hair follicle regression in cashmere goats. BMC Genomics 2018;19(1):222. https://doi.org/10.1186/s12864-018-4603-3 PMid: 29587631.
[60] Schlake T. Segmental Igfbp5 expression is specifically associated with the bent structure of zigzag hairs. Mech Dev 2005;122(9):988–97. https://doi.org/10.1016/j.mod.2005.04.012 PMid: 16024235.
[61] He XY, Hao H, Liu D, et al. Difference of microRNA expression in the ear and back skin of young alpaca (*Lama acos*). Chin J Biochem Mol Biol 2010;26(11):1016–22. https://doi.org/10.3724/SP.J.1142.2010.40466.
[62] Sur I, Unden AB, Toftgard R. Human Krüppel-like factor5/KLF5: synergy with NF-B/Rel factors and expression in human skin and hair follicles. Eur J Cell Biol 2002;81(6):323–34. https://doi.org/10.1078/0171-9335-00257 PMid: 12113473.
[63] Shyh-Chang N, Zhu H, Yvanka de Soysa T, et al. Lin28 enhances tissue repair by reprogramming cellular metabolism. Cell 2013;155(4):778–92. https://doi.org/10.1016/j.cell.2013.09.059 PMid: 24209617.
[64] Strahl BD, Allis CD. The language of covalent histone modifications. Nature 2000;403(6765):41–5. https://doi.org/10.1038/47412 PMid: 10638745.
[65] Frye M, Fisher AG, Watt FM. Epidermal stem cells are defined by global histone modifications that are altered by Myc-induced differentiation. PLoS One 2007;2(8):e763. https://doi.org/10.1371/journal.pone.0000763 PMid: 17712411.
[66] LeBoeuf M, Terrell A, Trivedi S, et al. Hdac1 and Hdac2 act redundantly to control p63 and p53 functions in epidermal progenitor cells. Dev Cell 2010;19(6):807–18. https://doi.org/10.1016/j.devcel.2010.10.015 PMid: 21093383.
[67] Sennett R, Wang Z, Rezza A, et al. An integrated transcriptome atlas of embryonic hair follicle progenitors, their niche, and the developing skin. Dev Cell 2015;34(5):577–91. https://doi.org/10.1016/j.devcel.2015.06.023 PMid: 26256211.
[68] Zhang J, Wallace SJ, Shiu MY, et al. Human hair follicle transcriptome profiling: a minimally invasive tool to assess molecular adaptations upon low-volume, high-intensity interval training. Physiol Rep 2017;5(23):e13534. https://doi.org/10.14814/phy2.13534 PMid: 29212859.
[69] Salzman J, Chen RE, Olsen MN, et al. Cell-type specific features of circular RNA expression. PLoS Genet 2013;9(9):e1003777. https://doi.org/10.1371/journal.pgen.1003777 PMid: 24039610.
[70] Hansen TB, Jensen TI, Clausen BH, et al. Natural RNA circles function as efficient microRNA sponges. Nature 2013;495(7441):384–8. https://doi.org/10.1038/nature11993 PMid: 23446346.
[71] Vanhoutteghem A, Delhomme B, Hervé F, et al. The importance of basonuclin 2 in adult mice and its relation to basonuclin 1. Mech Dev 2016;140:53–73. https://doi.org/10.1016/j.mod.2016.02.002 PMid: 26923665.
[72] Chen BK, Leiferman KM, Pittelkow MR, et al. Localization and regulation of pregnancy-associated plasma protein expression in healing human skin. J Clin Endocrinol Metab 2003;88(9):4465–71. https://doi.org/10.1210/jc.2003-030193 PMid: 12970325.
[73] Philpott MP, Sanders DA, Kealey T. Effects of insulin and insulin-like growth factors on cultured human hair follicles: IGF-I at physiologic concentrations is an important regulator of hair follicle growth *in vitro*. J Invest Dermatol 1994;102(6):857–61. https://doi.org/10.1111/1523-1747.ep12382494 PMid: 8006448.
[74] Nixon AJ, Ford CA, Oldham JM, et al. Localisation of insulin-like growth factor in skin follicles of sheep (*Ovis aries*) and during an induced growth cycle. Comp Biochem Physiol A Physiol 1997;118(4):1247–57. https://doi.org/10.1016/s0300-9629(97)00048-0 PMid: 9505430.
[75] Stenn KS, Paus R. Controls of hair follicle cycling. Physiol Rev 2001;81(1):449–94. https://doi.org/10.1152/physrev.2001.81.1.449 PMid: 11152763.
[76] Su R, Fan Y, Qiao X, et al. Transcriptomic analysis reveals critical genes for the hair follicle of Inner Mongolia cashmere goat from catagen to telogen. PLoS One 2018;13(10):e0204404. https://doi.org/10.1371/journal.pone.0204404 PMid: 30356261.
[77] Millar SE, Willert K, Salinas PC, et al. WNT signaling in the control of hair growth and structure. Dev Biol 1999;207(1):133–49. https://doi.org/10.1006/dbio.1998.9140 PMid: 10049570.
[78] Rishikaysh P, Dev K, Diaz D, et al. Signaling involved in hair follicle morphogenesis and development. Int J Mol Sci 2014;15(1):1647–70. https://doi.org/10.3390/ijms15011647 PMid:24451143.
[79] Assa-Kunik E, Torres IL, Schejter ED, et al. Drosophila follicle cells are patterned by multiple levels of notch signaling and antagonism between the notch and JAK/STAT pathways. Development 2007;134(6):1161–9. https://doi.org/10.1242/dev.02800 PMid: 17332535.
[80] Sordella R, Classon M, Hu KQ, et al. Modulation of CREB activity by the rho GTPase regulates cell and organism size during mouse embryonic development. Dev Cell 2002;2(5):553–65. https://doi.org/10.1016/s1534-5807(02)00162-4 PMid: 12015964.
[81] Sordella R, Jiang W, Chen G, et al. Modulation of Rho GTPase signaling regulates a switch between adipogenesis and myogenesis. Cell 2003;113(2):147–58. https://doi.org/10.1016/S0092-8674(03)00271-X PMid: 12705864.
[82] Zhang S, Zhang R, Wu F, et al. MicroRNA-208a regulates H9c2 cells simulated ischemia–reperfusion myocardial injury via targeting CHD9 through Notch/NF-kappa B signal pathways. Int Heart J 2018;59(3):580–8. https://doi.org/10.1536/ihj.17-147 PMid: 29681568.
[83] He J, Cai Y, Luo LM, et al. Expression of Wnt and NCX1 and its correlation with cardiomyocyte apoptosis in mouse with myocardial hypertrophy. Asian Pac J Trop Med 2015;8(11):930–6. https://doi.org/10.1016/j.apjtm.2015.10.002 PMid: 26614993.
[84] DasGupta R, Kaykas A, Moon RT, et al. Functional genomic analysis of the Wnt-wingless signaling pathway. Science 2005;308(5723):826–33. https://doi.org/10.1126/science.1109374 PMid: 15817814.
[85] Tang W, Dodge M, Gundapaneni D, et al. A genome-wide RNAi screen for Wnt/beta-catenin pathway components identifies unexpected roles for TCF transcription factors in cancer. Proc Natl Acad Sci U S A 2008;105(28):9697–702. https://doi.org/10.1073/pnas.0804709105 PMid:18621708.
[86] Mosimann C, Hausmann G, Basler K. Beta-catenin hits chromatin: regulation of Wnt target gene activation. Nat Rev Mol Cell Biol 2009;10(4):276–86. https://doi.org/10.1038/nrm2654 PMid: 19305417.
[87] Bai WL, Dang YL, Yin RH, et al. Differential expression of microRNAs and their regulatory networks in skin tissue of Liaoning Cashmere goat during hair follicle cycles. Anim Biotechnol 2016;27(2):104–12. https://doi.org/10.1080/10495398.2015.1105240 PMid: 26913551.